20056033

31 Effects of Inert Gases on Combustion Properties of Outwardly Propagating DME Flames

Kimitoshi TANOUE [1], Shuho MORI [1], Fumio SHIMADA [1]
[1] Oita University, Department of Mechanical Engineering
700 Dannoharu, Oita, Japan

The purpose of this study is to clarify the combustion properties of dimethyl ether (DME) and to develop a new combustion techniques with high efficiency and low emission for internal combustion engine operated by DME/O_2/Ar mixtures and DME/O_2/CO_2 mixtures. Combustion properties were elucidated in a spherical bomb by using schlieren images with a high-speed camera, for equivalence ratios ranging from 0.8 to 2.0 at an initial pressure of 1 atm and a temperature of 298 K. Unstretched laminar burning velocity and Markstein number were deduced and compared with the corresponding DME/Air mixtures.

Keywords : Premixed Combustion, Combustion Phenomena / DME/O_2/Ar, DME/O_2/CO_2

Burning Velocity, Flame Stretch, Markstein Number

1. INTRODUCTION

Recently, the environmental issues on an earth scale and the depletion of energy resources are requiring internal combustion engines to improve fuel economy and to reduce NOx emissions and particles urgently, which cause mainly atmospheric pollution. For this purpose, an alternative fuel and new combustion techniques have been studied so far [1]-[3]. Dimethyl ether (DME), which is one of the most promising alternative fuels with the lowest overall pollutant emissions and the most excellent fuel economy, have been paid attention as a potential alternative especially to diesel fuel. DME is an ether of a lowest molecular with a cetane number of 55-60, it has a excellent characteristics of spontaneous combustion as diesel fuel [4]-[6]. As the combustion properties of DME, however, differ from those of diesel fuel, it is necessary to investigate the combustion characteristics and the reaction process in detail for the proper application of DME to a new internal combustion engine.

As for the new combustion technique with high efficiency and low pollutant emission, the new diesel engine using Ar as the working gas was proposed to improve thermal efficiency [7]. Since a monatomic gas has a high specific heats ratio, using Ar as the working gas improves thermal efficiency, compared with air. In addition, Ar can be easily available. Furthermore, a flue gas recirculation (EGR) is usually used for internal combustion engines to reduce NOx emissions, and the combined combustion technique of EGR and pure oxygen combustion has been proposed for NOx free emission [8]. For these new combustion techniques, Ar and CO_2 play an important role in determining combustion properties, such as extinction and burning velocity. Therefore, the clarification of combustion properties of Ar and CO_2-dilution mixtures is important to specify the optimum running condition. In general, it is turbulent flames that occur in practical combustor, so modeling them in some way is needed to capture the phenomena quantitatively because of their complexities [9][10]. In this context, flamelet concept is important, because it is applicable to many turbulent flames in practice, including those in engines. Flamelet concept is based on the assumption that a chemical reaction occurs in thin layer that are convected and distorted by the turbulent flow field, while its structure still remain that of laminar flame. In this case, since turbulent flames can be considered as the assembly of laminar flamelets, quantitative study regarding the combustion properties of laminar flames, especially, stretched laminar flames are important for turbulent combustion modeling. In past studies [11], we have investigated the combustion properties of DME/Air laminar flames over a wide range of equivalence ratio. The effects of flame stretch was quantified for outwardly propagating flames, and quantitative explanation regarding its combustion mechanisms was given in terms of the interaction between Lewis number effects and flame stretch. In this study, the combustion properties of DME/O_2/Ar mixtures and DME/O_2/CO_2 mixtures, are investigated and compared with those of DME/Air mixtures for developing new combustion techniques.

2. EXPERIMENT AND CALCULATION

2.1 COMBUSTION CHAMBER

The combustion chamber [11]-[13] used in this study was a nearly spherical vessel with a mean inner diameter of about 100 mm and a total volume of about 2000cm^3. It was provided with four 92 mm diameter transparent windows at four sides for flame observation, and two 92 mm diameter perforated plates at two opposite sides. A cross-sectional view of the combustion chamber observed from the direction of one of the transparent windows is shown in Fig. 1. A fan was installed behind each perforated plate to mix gases. The combustible mixture was spark-ignited at the center of the chamber using the minimum spark ignition energy to avoid ignition disturbances. Once

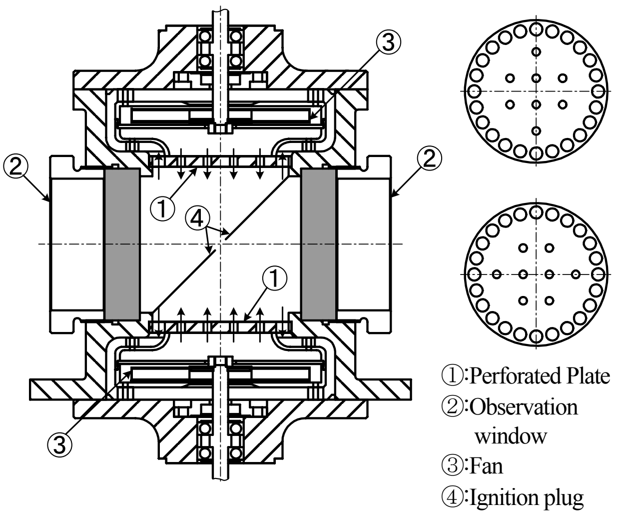

Fig. 1 Combustion Chamber

combustion was complete, the chamber was vented and flushed with air to remove condensed water vapor and to cool the system to the allowable initial temperature range of the experiment (298±3K). The flames were observed using the schlieren system with a high speed camera (1000 pictures per second). A schlieren image was recorded up to the instant where any part of it reached the edge of the viewing window in the bomb. The high-speed camera had a field-of-view of 72 × 77 mm (240pixels × 256 pixels) at a resolution of 0.3 mm/pixel, which is estimated to be enough to resolve flames with a radius ranging from 3 mm to 35 mm. For this range, pressure increases were found to be less than 0.7 % of the initial pressure. Similar to other work [11]-[13], measurements were limited to $\delta_T^0 / r < 2$ % so that the effects of curvature and transient phenomena associated with large flame thicknesses were small. Finally, radiative heat loss was small due to the large flame speeds, and was therefore ignored.

2.2 NUMERICAL CALCULATION METHOD

In this study, CHEMKIN software [14], which was originally developed by Sandia National Laboratories, was used to analyze the flames numerically. For calculation of one dimensional planar flames, the numerical code used was the PREMIX program [14] Details of this code are provided in the references [14]. The reaction mechanism used is based on that developed by Curran [15], to which the following two reactions related to Ar were added from GRI-Mech 3.0 [16].

$$H + O_2 + Ar \Leftrightarrow HO_2 + Ar \quad (1)$$

$$CH_2(S) + Ar \Leftrightarrow CH_2 + Ar \quad (2)$$

In order to predict the flame response to aerodynamic flame stretch, the OPPDIF code [14] was used. This code employs a set of one-dimensional conservation equations for counter-flow flames along the line of symmetry using a similarity transformation, assuming a specific form of the radial velocity profile. Details of the OPPDIF similarity solution are also provided in the reference [14]. In this configuration, combustible mixtures with specified compositions were injected through two nozzles to generate symmetric back-to-back planar stretched premixed flames. One of the flames was chosen for investigation. The flame properties required for analysis were specified as follows. To avoid ambiguity arising from the choice of spatial location, stretched laminar burning velocity, S_u was determined from

Table 1 Properties of mixtures

Group I

Composition	ϕ	Z (%vol.)	T_{ad} [K]	ρ_b/ρ_u	α [mm²/s]	D [mm²/s]	S_u^0 [cm/s]	L_u [mm]	Ma	Le
DME/Air	0.8	21.0	2484	0.136	20.3	12.6	30.7	0.2527	3.83	1.61
	0.9	21.0	2596	0.127	20.1	12.6	36.9	0.1770	3.24	1.60
	1.0	21.0	2666	0.121	19.9		41.5	0.1429	2.98	
	1.1	21.0	2693	0.119	19.8	19.3	44.0	0.1248	2.78	1.02
	1.2	21.0	2675	0.119	19.6	19.3	42.3	0.0900	1.94	1.02
	1.3	21.0	2628	0.120	19.4	19.2	37.3	0.0495	0.95	1.01
	1.4	21.0	2562	0.121	19.3	19.2	31.6	0.0415	0.68	1.01
	1.5	21.0	2499	0.122	19.1	19.1	22.9	−0.0157	−0.19	1.00
	1.6	21.0	2438	0.123	18.9	19.0	17.6	−0.0430	−0.40	1.00
	1.7	21.0	2362	0.125	18.8	19.0	12.4	−0.0746	−0.49	0.99
	1.8	21.0	2308	0.126	18.7	18.9	9.1	−0.0967	−0.47	0.99
	1.9	21.0	2243	0.128	18.5	18.9	6.4	−0.1315	−0.46	0.98
	2.0	21.0	2182	0.129	18.4	18.8	5.4	−0.1406	−0.42	0.98
DME/O_2/Ar	1.0	11.9	2666	0.135	19.6		22.7	0.3288	3.80	
	1.1	12.0	2697	0.134	19.5	19.6	27.8	0.2183	3.11	0.99
	1.2	11.8	2674	0.138	19.4	19.6	29.3	0.1925	2.91	0.99

DME/O_2/Ar (S_u^0,L_u and Ma shows numerical results.)	0.8	11.8	2484	0.156	19.9	11.9	17.4	0.3004	2.62	1.67
	0.9	11.8	2597	0.143	19.8	11.9	24.4	0.2658	3.28	1.66
	1.0	11.9	2666	0.135	19.6		30.4	0.2154	3.35	
	1.1	12.0	2697	0.134	19.5	19.6	34.3	0.1562	2.82	0.99
	1.2	11.8	2674	0.138	19.4	19.6	33.8	0.1438	2.51	0.99
	1.3	11.7	2628	0.141	19.3	19.6	30.9	0.1242	2.00	0.99
	1.4	11.6	2563	0.144	19.2	19.5	24.8	0.0906	1.17	0.98
	1.5	11.6	2499	0.146	19.0	19.5	17.9	0.0451	0.42	0.98
	1.6	11.7	2438	0.148	18.9	19.4	11.1			0.97
	1.7	11.6	2363	0.151	18.8	19.4	7.7	0.0462	0.20	0.97
	1.8	11.7	2307	0.153	18.7	19.4	6.3	0.0876	0.29	0.97
	1.9	11.7	2243	0.156	18.6	19.3	5.1			0.96
	2.0	11.7	2182	0.158	18.5	19.3	4.2			0.96
DME/O_2/CO_2 (S_u^0,L_u and Ma shows numerical results.)	0.8	34.9	2484	0.123	13.1	9.9	35.0	0.0749	1.94	1.33
	0.9	36.0	2596	0.115	13.0	9.9	44.0	0.0681	2.30	1.32
	1.0	36.8	2665	0.109	13.0		49.9	0.0483	2.00	
	1.1	37.0	2698	0.105	12.9	16.4	51.8	0.0446	1.79	0.79
	1.2	35.7	2672	0.105	12.7	16.3	47.0	0.0438	1.62	0.78
	1.3	34.6	2627	0.105	12.6	16.2	41.8	0.0293	0.97	0.78
	1.4	33.9	2561	0.107	12.5	16.2	36.4	0.0267	0.78	0.77
	1.5	33.8	2498	0.107	12.4	16.1	31.5	0.0053	0.14	0.77
	1.6	33.9	2439	0.108	12.3	16.1	26.3			0.77
	1.7	34.0	2365	0.109	12.2	16.0	20.6	−0.0394	−0.66	0.76
	1.8	34.3	2309	0.109	12.2	16.0	15.9	−0.0692	−0.91	0.76
	1.9	34.5	2243	0.110	12.1	15.9	11.5	−0.0925	−0.88	0.76
	2.0	34.8	2183	0.110	12.0	15.9	9.1	−0.0939	−0.73	0.76

Group II

Composition	ϕ	Z (%vol.)	T_{ad} [K]	ρ_b/ρ_u	α [mm²/s]	D [mm²/s]	S_u^0 [cm/s]	L_u [mm]	Ma	Le
DME/O_2/Ar	0.8	14.3	2654	0.138	19.7	11.9	29.4	0.2323	3.47	1.65
	0.9	14.3	2740	0.130	19.5	11.9	33.7	0.1618	2.79	1.64
	1.0	14.3	2794	0.124	19.4		39.3	0.1151	2.33	
	1.1	14.3	2821	0.122	19.2	19.6	42.5	0.0803	1.78	0.98
	1.2	14.3	2824	0.123	19.1	19.6	44.8	0.0691	1.62	0.97
	1.3	14.3	2803	0.125	18.9	19.5	43.0	0.0491	1.12	0.97
	1.4	14.3	2758	0.127	18.8	19.5	37.5	0.0243	0.48	0.97
	1.5	14.3	2701	0.129	18.7	19.5	32.7	0.0192	0.34	0.96
	1.6	14.3	2638	0.131	18.5	19.4	26.7	−0.0264	−0.38	0.96
	1.7	14.3	2562	0.133	18.4	19.3	19.6	−0.0652	−0.69	0.95
	1.8	14.3	2498	0.135	18.3	19.3	15.0	−0.0893	−0.73	0.95
	1.9	14.3	2426	0.138	18.1	19.2	11.5	−0.1157	−0.74	0.94
	2.0	14.3	2356	0.140	18.0	19.2	8.8	−0.1392	−0.68	0.94

$S_u = (\rho_b/\rho_u) \times S_b$, in which the flame speed relative to the burned gas, S_b, is defined as the axial flow velocity at the point of the maximum heat release rate, ρ is the mixture density, and the subscripts u and b denote properties associated with the unburned and burned mixtures, respectively. In this study, flame stretch, κ, was defined as the maximum axial velocity gradient ahead of the preheat zone [17]. Together with S_u, the laminar flame thickness, δ_T^0, is also an important flame property, because it yields the characteristic residence time within the flame. In this paper, the δ_T^0 for a mixture is calculated based on the thermal theory $\delta_T^0 = \alpha / S_u^0$, where α is the thermal diffusivity of the mixture and S_u^0 is the unstretched laminar burning velocity. In addition, equilibrium calculation was conducted using the EQUIL code [14], and all thermodynamic and transport properties were also evaluated by the CHEMKIN code [14].

2.3 PROPERTIES OF MIXTURES

The mixtures used in this study were DME/O_2/Ar mixtures and DME/O_2/CO_2 mixtures. The composition is given by the following equation.

$$CH_3OCH_3 + X_0 O_2 + X_1 (N_2 \text{ or Ar or } CO_2), \quad (3)$$

where X_0 is the number of moles of oxygen per one mole of fuel in a mixture, X_1 is the number of moles of dilution per one mole of fuel in a mixture. In this case, the equivalence ratio, ϕ, can be calculated as follows.

$$\phi = \frac{3}{X_0} . \tag{4}$$

Moreover, dilution ratio, Z, was used to specify the degree of dilution, which can be defined as follows.

$$Z = \frac{X_0}{X_0 + X_1} . \tag{5}$$

In this study, the mixtures can be divided into two groups, that is, Group Ⅰ consists of DME/O_2/Ar mixtures and DME/O_2/CO_2 mixtures having the same adiabatic flame temperature as that of the corresponding DME/Air mixtures at each equivalence ratio, which can be prepared by changing dilution ratio, Z. These mixtures were used to elucidate the effect of the kind of inert gas on the combustion properties. Group Ⅱ consists of DME/O_2/Ar mixtures with Z=14.3%. These were used to elucidate the effect of the amount of dilution on the combustion properties.

Table 1 shows the properties of the mixtures on Group Ⅰ and Ⅱ, respectively. In Table 1, T_{ad} is the adiabatic combustion temperature, ρ_b/ρ_u is the ratio of the burned to unburned gas density, α is the thermal diffusivity, D is the diffusion coefficient of the deficient reactant, S_u^0 is the unstretched laminar burning velocity, L_u is the Markstein length and Ma is the Markstein number. T_{ad}, and ρ_b/ρ_u were calculated by the EQUIL code, S_u^0, L_u and Ma were obtained by experiment. The numerical results of S_u^0, L_u and Ma of DME/O_2/Ar mixtures and DME/O_2/CO_2 mixtures on Group Ⅰ are also shown for comparison. Moreover, Le is the Lewis number based on the molecular diffusion coefficient of the deficient reactants.

3. MEASUREMENTS OF LAMINAR BURNING VELOCITY

In this chapter, the method for analyzing experimental data accurately is discussed. Effects of flame stretch on the laminar burning velocities were correlated using an early proposal of Markstein [18] that was subsequently generalized and extended at the limit of small stretch, as discussed by Clavin [19], as follows:

$$S_u = S_u^0 - L_u \kappa , \tag{6}$$

where S_u^0 is the stretched laminar burning velocity, κ is the stretch rate. The unstretched laminar burning velocities, S_u^0, were determined by linear extrapolation of the measured stretched laminar burning velocity to zero stretch rate [17]. In the process, the effects of the measurement error on the laminar burning velocity and Markstein number were investigated as follows. The error regarding the least square method is estimated by the following equations [20].

$$Error(S_u) = \sqrt{\frac{\sum_{i=1}^{N} \left[S_{ui} - \left(S_u^0 - L_u \kappa_i \right) \right]^2}{N}} , \tag{7}$$

$$Error(L_u) = \sqrt{\frac{\sum_{i=1}^{N} \left[\frac{S_{ui}}{\kappa_i} - \frac{1}{\kappa_i} \left(S_u^0 - L_u \kappa_i \right) \right]^2}{N}} , \tag{8}$$

where S_{ui} is the burning velocity and κ_i is the stretch rate obtained by *ith* measurement, respectively.

Fig. 2 shows one example of experimental results of S_u^0 and L_u. From this figure, it is found that the measurement accuracy is within 3%. For all the mixtures, the measurement accuracy was found to be within 10% at most. Once S_u^0 and L_u are specified, Markstein number, Ma, can be obtained by the following equation.

$$Ma = \frac{S_u^0 \times L_u}{\alpha} . \tag{9}$$

Table 1 shows experimental data for DME/O_2/Ar and DME/O_2/CO_2 obtained by the method mentioned above and data for DME/Air provided in the reference [11].

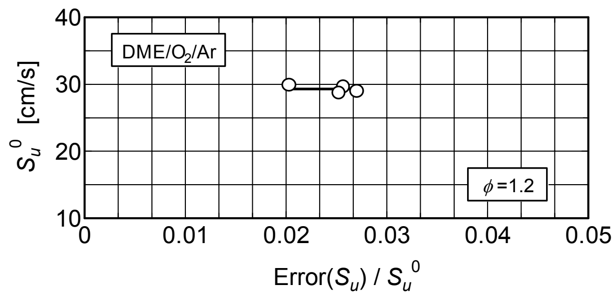

(a) Error of S_u^0

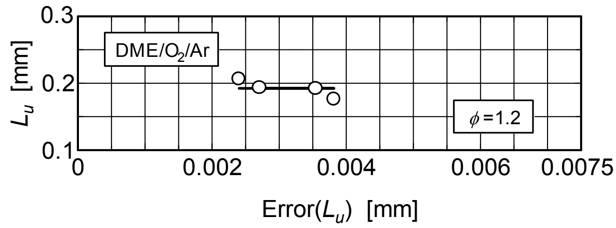

(b) Error of L_u

Fig. 2 Effects of the Error of measurements on the combustion properties

4. RESULTS AND DISCUSSION

4.1 EFFECTS OF INERT GAS ON LAMINAR BURNING VELOCITY

Firstly, in this study, the effects of inert gas on the laminar burning velocity were investigated. Fig. 3 (a) shows the experimental and numerical results of unstretched laminar burning velocity, S_u^0, of DME/Air mixtures, DME/O_2/Ar mixtures and DME/O_2/CO_2 mixtures on Group 1, along with the data for DME/Air reported by Daly et al. [21] and Zhao et al. [22]. It can be seen from Fig. 3 (a) that the data reported by Daly et al. give good agreement with the present data, while the data reported by Zhao et al. and numerical results overestimate the burning velocity for all equivalence ratios. The higher burning velocities reported by Zhao et al. may be due to the fact that they used a counter-flow twi-flame technique, in which the data correction procedure is still the subject of debate. Fig. 3 (a) also shows that the burning velocities obtained from the PREMIX show very good agreement with the data of Zhao et al. This is due to the fact that the reaction mechanism employed in this study has been developed based

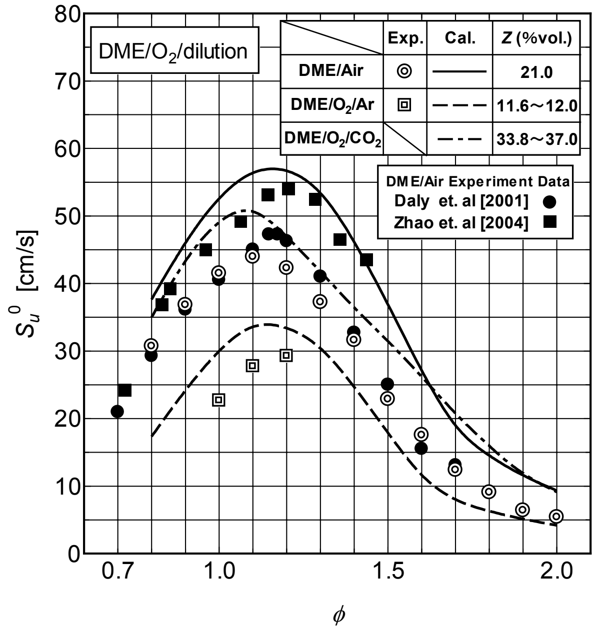

(a) Group Ⅰ

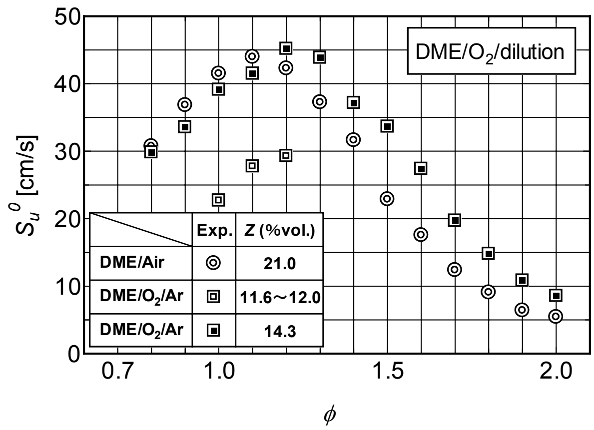

(b) Group Ⅱ

Fig. 3 Variations of S_u^0 with ϕ

on the data of Zhao et al. For DME/O_2/Ar mixtures, numerical results also give higher burning velocities than experimental results for equivalence ratios from 1.0 to 1.2. The burning velocities, however, of DME/O_2/Ar mixtures for equivalence ratios richer than 1.3 and those of DME/O_2/CO_2 mixtures for all equivalence ratios could not be measured correctly, because cellularity was found to trigger at a very early stage. It can be seen from the comparison of calculation results for DME/Air mixtures, DME/O_2/Ar mixtures and DME/O_2/CO_2 mixtures that DME/Air mixtures have the highest burning velocities and DME/O_2/Ar mixtures have the lowest burning velocities. According to thermal theory of Mallard and Le Chatelier [23], laminar burning velocity depends mainly on the thermal diffusivity, α, and mass production rate of the fuel, $\dot{m}_F$. That is;

$$S_u^0 \propto \sqrt{\alpha \cdot \frac{\dot{m}_F}{\rho}} \quad . \tag{10}$$

Mass production rate of the fuel, $\dot{m}_F$ [kg/(m^{3}s)], can be expressed by fuel production rate, $\dot{\omega}_F$ [Kmol/(m^{3}s)], and fuel molecular weight , M_{WF}. That is;

$$\dot{m}_F = \dot{\omega}_F MW_F \quad . \tag{11}$$

Assuming one-step irreversible overall reaction of Arrhenius form, $\dot{\omega}_F$ can be given by

$$\dot{\omega}_F \equiv \frac{d[X_F]}{dt} = A[X_F]^m [X_{ox}]^n \exp(E_A/RT), \tag{12}$$

where A is frequency factor, X_F and X_{ox} are the fuel and Oxidation mole concentration, respectively, E_A is the activation energy, R is the specific gas constant, and m and n is the reaction order. It is found from Eqs. (10)-(12) that burning velocity depend mainly on (1) the thermal diffusivity α, and (2) the concentrations of fuel and oxidation for the same fuel at a given temperature. Compared DME/Air mixtures with DME/O_2/CO_2 mixtures, the latter have small thermal diffusivities, which leads to their lower burning velocities, as shown in Fig. 3(a). On the other hand, compared DME/Air mixtures with DME/O_2/Ar mixtures, although both have almost the same thermal diffusivities, the latter have lower burning velocities. This is due to their lower concentration of DME and O_2, in a mixture, because Ar has lower specific heat than N_2, so the larger amount of Ar is needed to keep the temperatures of DME/O_2/Ar mixtures the same as those of the corresponding DME/Air mixtures.

Fig. 3 (b) shows the comparison between DME/O_2/Ar mixtures on Group Ⅰ and Group Ⅱ, along with the data of DME/Air mixtures. It can be seen from Fig. 3 (b) that DME/O_2/Ar mixtures on Group Ⅱ have almost the same laminar burning velocities on the lean side and a little bit higher values on the rich side, compared with DME/Air mixtures. In this case, DME/O_2/Ar mixtures on Group Ⅱ have about 6% higher flame temperatures.

4.2 EFFECTS OF INERT GAS ON FLAME INSTABILITY

As flames gets instable, cellular flames triggers. Then the flame surface area increases, which leads to a increase in the burning velocity. This can affect the system performance of an engine. There are two types of instabilities [19]. The first is called the hydrodynamic instability and is caused by the density change across a flame. The second instability is due to differential diffusion of reactants and energy, and is called the thermal-diffusive instability. The thermal-diffusive instability occurs when the Lewis number is less than some critical value, which can be realized by changing a kind of inert gas. Therefore, the effect of inert gas on unstable of flame was investigated.

Fig. 4 (a) (b) (c) show schlieren image for DME/Air mixture, DME/O_2/Ar mixtures and DME/O_2/CO_2 mixtures on Group Ⅰ, respectively. In Fig. 4 (a), DME/Air flames are found to be stable for all equivalence ratios. On the other hand, in Fig. 4 (b), DME/O_2/Ar flames are found to get unstable for equivalence ratios richer than 1.3, while they are found to remain stable for equivalence ratios smaller than 1.2. This can be due to their smaller Lewis number on the richer side. Considering that DME/Air mixtures and DME/O_2/Ar mixtures have almost the same values of Lewis number at each equivalence ratio, the different response to flame instability between them are due to their different chemical reaction times. That is, DME/O_2/Ar mix-

(φ=0. 8, t=12ms)　(φ=1. 6, t=14ms)　(φ=1. 8, t=18ms)

(a) DME/Air

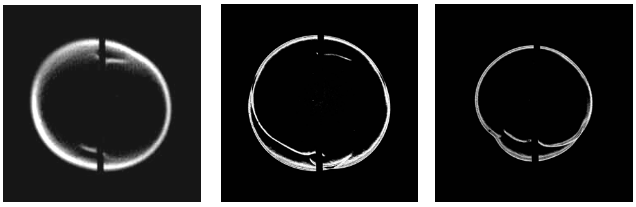

(φ=1. 0, t=17ms)　(φ=1. 6, t=14ms)　(φ=1. 8, t=20ms)

(b) $DME/O_2/Ar$

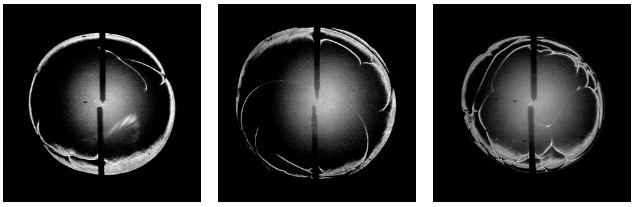

(φ=0. 8, t=10ms)　(φ=1. 6, t=8ms)　(φ=1. 8, t=8ms)

(c) $DME/O_2/CO_2$

Fig. 4 Schlieren Photographs of Laminar Flames for Group Ⅰ

tures have lower burning velocities than DME/Air mixtures, so that they have longer chemical reaction times which are considered to be enough to make the flame unstable. It can be seen from Fig. 4 (c) that $DME/O_2/CO_2$ flames are the most unstable. This could be due to the fact that they have the lowest Lewis numbers for all equivalence ratios.

Next, in this study, the quantitative effects of the flame instability on laminar burning velocity were investigated. Fig. 5 shows variations of stretched laminar burning velocity, S_u, as a function of flame radius, r, for DME/Air mixtures and $DME/O_2/CO_2$ mixtures with equivalence ratios of 0.8 and 1.6, respectively. It can be seen from Fig. 5 that $DME/O_2/CO_2$ mixtures have higher burning velocities at both equivalence ratios, even though they have lower unstretched laminar burning velocities calculated by PREMIX, as can be seen in Fig. 3. This is due to the increase in the surface area caused by the instability for $DME/O_2/CO_2$ flames. Therefore, it follows that the effects of flame instability on burning velocity are qualitatively large.

4.3 EFFECTS OF INERT GAS ON STRETCHED LAMINAR FLAME

Fig. 6 (a) shows both experimental and numerical results for Markstein number, Ma, as a function of equivalence ratio, ϕ, on Group Ⅰ, suggesting that the values of Ma decrease with increasing equivalence ratio for all mixtures, although there are some quantitative deviations between experimental results and numerical results. Compared DME/Air mixtures with $DME/O_2/CO_2$ mixtures, the latter are found to have lower values of Ma for all equivalence ratios. This can be explained in terms of the interaction between flame stretch and the Lewis

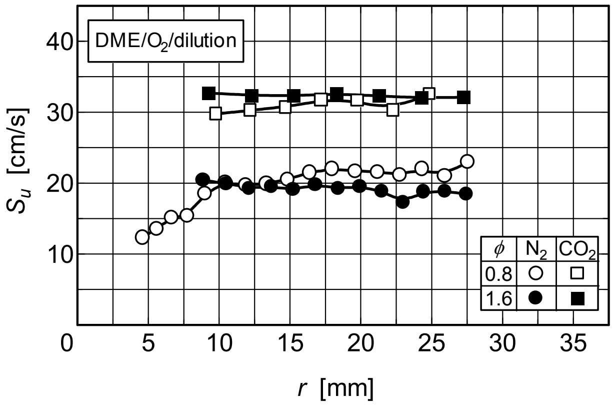

Fig. 5 Variations of S_u with r

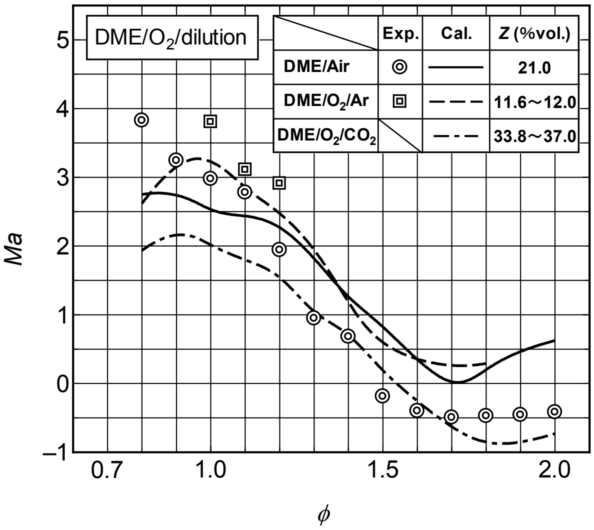

(a) Group Ⅰ

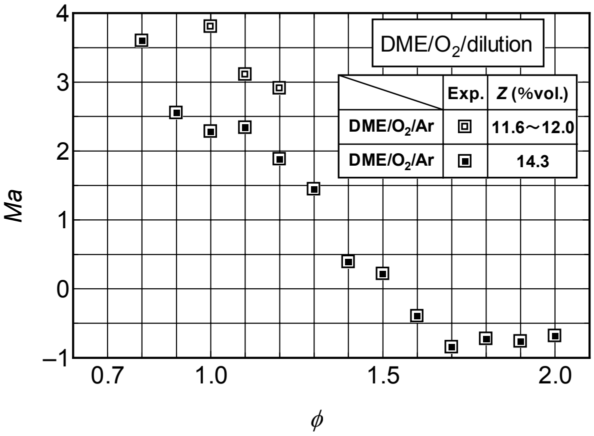

(b) Group Ⅱ

Fig. 6 Variations of Ma with ϕ

number effect, as described below. That is, for a two-reactant mixture and a single-step reaction, the Clavin and Williams' asymptotic analysis yields [19] the following.

$$Ma = \frac{\sigma}{\sigma-1}\ln\sigma + \frac{\beta(Le-1)}{2}\frac{1}{\sigma-1}\int_0^{\sigma-1}\frac{\ln(1+x)}{x}dx \,, \qquad (13)$$

where σ is the density ratio ($=\rho_u/\rho_b$), β is the Zeldovich number, *Le* is Lewis number and *x* is a dummy variable. From Eq. (13), it is found over a wide range of mixtures, *Ma* changes in a nearly linear fashion with *Le*. In Table 1, it can be seen that DME/O_2/CO_2 mixtures have small Lewis numbers, compared with the corresponding DME/Air mixtures. This is mainly due to the smaller thermal diffusivities of DME/O_2/CO_2 mixtures. That is, the decrease in thermal diffusivity by CO_2 dilution lowers the Lewis number, leading to decrease in Markstein number, compared to the corresponding DME/Air mixtures. Compared DME/Air mixtures with DME/O_2/Ar mixtures, the latter are found to have lower values of *Ma* for equivalence ratios from 0.8 to 1.3. In Table 1, it can be seen that DME/O_2/Ar mixtures have large Lewis numbers for equivalence ratios from 0.8 to 1.3, compared with the corresponding DME/Air mixtures. This is mainly due to the smaller mass diffusion of reactants in a DME/O_2/Ar mixture. That is, the decrease in the mass diffusion of reactants by Ar dilution increases the Lewis number, leading to increase in Markstein number, compared to DME/Air mixtures. On the other hand, both are found to have the similar Lewis numbers for equivalence ratios richer than 1.3, which results in the similar values of Markstein numbers.

Fig. 6 (b) shows the comparisons of Markstein numbers of DME/O_2/Ar mixtures between Group Ⅰ and Group Ⅱ. It can be seen from Fig. 6 (b) that DME/O_2/Ar mixtures on Group Ⅱ, which have smaller amounts of Ar, have smaller Markstein numbers, compared with the corresponding DME/O_2/Ar mixtures on Group Ⅰ. This may be due to the lower Lewis number of DME/O_2/Ar mixtures on Group Ⅱ, as can be seen in Table1. That is, as Ar has larger thermal diffusivity than DME, the thermal diffusivity of a mixture decreases with decreasing amounts of Ar, which leads to decrease in Lewis number and Markstein number for Group Ⅱ mixtures.

5. CONCLUSIONS

In this study, the following conclusions were obtained.

1. Compared DME/Air mixtures, DME/O_2/Ar mixtures and DME/O_2/CO_2 mixtures, which have the same adiabatic flame temperature at each equivalence ratio, DME/Air mixtures were found to have the highest burning velocities and DME/O_2/Ar mixtures have the lowest burning velocities.
2. From schlieren image, DME/Air flames were found to be stable for all equivalence ratios. On the other hand, DME/O_2/Ar flames were found to get unstable for equivalence ratios richer than 1.3, while they were found to remain stable for equivalence ratios smaller than 1.2. In addition, DME/O_2/CO_2 flames were found to be the most unstable, and the effects of flame instability on burning velocity were qualitatively large.
3. Markstein number decrease with increasing equivalence ratio for all mixtures. This behavior can be explained in terms of the interaction between flame stretch and the Lewis number effect.

ACKNOWLEDGEMENTS

This work was partially supported by Grant-in-Aid for Science Research No.16760159 from the Ministry of Education, Science and Culture of Japan, the Suzuki Foundation and the Nissan Science and Technology Corporation. The authors thank Prof. Moriyoshi of the Chiba University, Prof. Konno and Prof. Chen of the Ibaragi University for their useful advises. We would like to thank Mr. Hirota, Mr. Kawano, Mr. Hara and Mr. Miyahara for their help with the experiments.

REFERENCES

[1] Heywood, J.B.: Internal Combustion Engine Fundamentals, McGraw-Hill, (1988), 930p

[2] Bradley, D., Lawes, M., and Sheppard, C. G. W. : Proc. Instn. Mech. Engrs., Vol.214, part C, (2001), pp.257-268

[3] Takagi, Y. : Proc. Combust. Inst. 27, (1998), pp.2055-2068

[4] T. H. Fleisch et al.: Soc. Am. Engrs. Paper SAE-950061

[5] B., J. Hansen, et al.: Soc. Am. Engrs. Paper SAE-950063

[6] E. D. Larson, R. Tingjin,: Energy Sustain, Develop. Ⅶ(4), (2003), pp.2-44

[7] Takahashi, M : Combustion Study, Vol.115, (1999), pp.43-53

[8] Ruan, J. Kobayashi, H., and Nioka, T.: Combust. Flame, Vol.124(2001), pp.225-230

[9] Bradley, D. : Proc. Combust. Inst. 24(1992), pp.247-262

[10] Peters, N. : Turbulent Combustion, Cambridge Univ. Press, (2000)

[11] Tanoue, K. et al. : Reviews of Automotive Engineering, Vol.2(2005), pp.129-136

[12] Tanoue, K., et al. : JSME Int. J. Series B, Vol.46, (2003), pp.416-424,

[13] Tanoue, K. : Proc. The 6th ASME-JSME Thermal Engineering Joint Conference, CD-ROM (2003), 7p

[14] Kee, R.J., Rupley, F.M. and Miller, J.A. et al.: CHEMKIN Collection, Release 3.7, Reaction Design, Inc., San Diego, CA(2003)

[15] Kaiser, E.W., et al. : Int. J. Phys. Chem. 3A104 : 8194-8206 (2000)

[16] http://www.me.berkeley.edu/gri_mech/

[17] Law, C. K., and Sung, C. J.: Pro. Energy Combust. Sci., Vol.26(2002), pp.459-505

[18] Markstein, G.H. : Non-steady Flame Propagation, Pergammon, Oxford, (1964)

[19] Clavin, P.: Prog. Energy Combust. Sci., Vol.11(1985), pp.1-59

[20] Huang, Y., Sung, C.J., and Eng, J.A.: Combust. Flame, Vol.139(2004), pp.239-251.

[21] Daly, C. A., Simmie, J. M., et al.: Combust. Flame, Vol.125(2001), pp.1329-1340

[22] Zhoa, Z., Kazakov, A., and Dryer, F. L.: Combust. Flame, Vol.139(2004), pp.52-60

[23] Turns, S. R. : An Introduction to Combustion, McGraw-Hill, （2000）, pp.253-300.